JOURNAL OF MATERIALS SCIENCE 30 (1995) 2526–2530

Effect of grain size on the martensitic transformation in NiTi alloy

F. J. GIL, J. M. MANERO, J. A. PLANELL
Departamento Ciencia de los Materiales e Ingeniería Metalúrgica, ETS Ingenieros Industriales de Barcelona, Universidad Politécnica de Catalunya, Diagonal 647, 08028 Barcelona, Spain

The effect of grain size on the martensitic transformation in Ni42Ti shape memory alloy has been studied. The kinetics of grain growth has been evaluated and the influence of different grain sizes on the transformation temperatures and the thermodynamic magnitudes has been reported. Image analysis and flow calorimetry techniques have been used. The study shows that grain boundaries favour the martensitic transformation and at the same time obstruct retransformation. Enthalpy and entropy variations are independent of grain size, but elastic energy decreases with the grain size.

1. Introduction

The determination of transformation temperatures and thermodynamic values and their relation to grain size is particularly useful when choosing a particular alloy for a specific practical shape memory application at a well defined working temperature. In the present work, martensitic transformation parameters have been studied in relation to grain growth for different heat treatment temperatures and times.

The driving force for grain growth comes from the surface energy of the grain boundaries. When thermal energy is given to the material, diffusion takes place which leads to grain selection. This means that the number of grains decreases, their size increases, the area of the grain boundaries decreases, the total energy stored in them decreases and, consequently, a state of higher thermodynamic stability is reached [1–4].

The experimental model formulated by Beck *et al.* [5–7] for normal grain growth of single phase metals states that

$$D - D_o = Kt^n \quad (1)$$

where D is the size of the grain at a certain time, D_o is the initial grain size, t is the time of heat treatment and K and n are constants which depend on the metal composition and the temperature, but are independent of the grain size. Moreover, if atomic diffusion across a grain boundary is taken as a simple activated process, it can be demonstrated that the constant K in Equation 1 can be written in terms of temperature as

$$K = K_o \exp(-Q_g/RT) \quad (2)$$

where K_o is a constant in which the specific interfacial energy of the grain boundary is included, Q_g is the activation energy of the process, T is the temperature in Kelvin and R is the gas constant.

The effect of grain size and grain boundaries on the martensitic transformation, particularly on the transformation temperatures, has been studied in alloys exhibiting shape memory effect. Martensite formation can be initiated by cooling the material below M_s, defined as the temperature at which the martensitic transformation begins. M_f is the temperature at which the martensitic transformation finishes. The transformation is reversible, with A_s the temperature at which the reverse austenetic transformation (martensite → austenite) begins upon heating, and A_f the temperature at the end of the reverse austenitic transformation. The evolution of these temperatures, especially of the martensitic starting transformation temperature, M_s, has been usually interpreted in terms of strengthening of the austenitic phase and/or increasing the non-chemical energy terms opposing the transformation, when grain size reduces. These points have also been taken for the analysis of non-thermoelastic martensitic transformations, although they have not always been discussed quantitatively [8–9].

The thermodynamic study was performed according to the recent model proposed by Ortin and Planes [10] for the thermoelastic martensitic transformation, which provides the possibility of its evaluation by means of calorimetric data [11].

In the direct exothermic (austenite → martensite) transformation, part of the latent heat generated, $-\Delta H_{chem}$ is stored as elastic energy, ΔH_{el}, and part is absorbed as friction energy, E_{fr}, therefore the average heat is

$$-Q = -\Delta H_{chem} - \Delta H_{el} + E_{fr} \quad (3)$$

In the reverse (martensite → austenite) transformation, while ΔH_{chem} is absorbed by the sample, ΔH_{el} is reversibly recovered. However, work, E_{fr}, is necessary in order to overcome friction which hinders the regression of the interphases.

0022–2461

The average heat measured is

$$Q = \Delta H_{chem} - \Delta H_{el} + E_{fr} \quad (4)$$

The hypotheses of this model are that friction energy represents only work and it does not transform into heat, and that variation of specific heat at constant pressure between the matrix and martensitic phase is neglected.

2. Experimental procedure

This study was carried out on polycrystalline samples of Ni42Ti (weight percentage) with austenitic phase at room temperature. Twenty slices of 4 mm in diameter and 3 mm in thickness, were cut from a single bar. Two of these samples were used as reference specimens, while the remaining 18 were given different heat treatments at 900, 1000 and 1100 °C during 5, 10, 15, 30, 60 and 120 min, respectively, at each temperature.

A set of specimens was placed in the furnace at the fixed temperature for each experiment and then taken from the furnace after the appropriate time of heat treatment and quenched in water at 20 °C, which gave the same cooling rate for all the samples.

The specimens were then prepared for metallographic observation. Grain size parameters (perimeter, area and average diameter) were obtained using image analysis techniques, by means of a microm image processing (MIP) apparatus. After optimizing the image, by improving the contrast and using pseudocolour representation, the parameters which had to be evaluated were identified: perimeter, area and average diameter of each grain of the polycrystal. The quantified values were then listed.

The transformation temperatures for the samples were measured during the heating and cooling cycles. The flow calorimeter measures differential signals, ΔT, by means of Melcor thermobatteries consisting of 32 thermocouples of p–n junctions made of Bi–Te–Se–Sb quaternary alloys connected in opposition. These thermobatteries have a working range from − 150 up to 100 °C. Temperature was measured by means of a standard Pt-100 probe. All signals were digitized through a multichannel recorder and linked to a microcomputer. The sensitivity of this calorimetric technique is approximately 100 times higher than other conventional methods such as differential thermal analysis (DTA) or differential scanning calorimetry (DSC) [12, 13].

The M_s and austentitic A_s, starting transformation temperatures can be determined when there is a sudden increase in the calorimetric signal, while the finish temperatures, M_f and A_f, are determined when the calorimetric signal returns to the baseline. The transformation temperatures of the heat treated specimens were measured during the first heating and cooling cycle. No significant differences from these values were found when the sample was thermally cycled several times.

The heat absorbed or released during the transformation is determined by measuring the area below the curve. The entropy is obtained by integration of the mean heat differential with respect to the temperature. The average chemical energy variation between the direct and the reverse transformation is calculated as

$$\Delta H_{chem} = T_o \overline{\Delta S} \quad (5)$$

where $\overline{\Delta S}$ is the average entropy variation between transformation and retransformation, and T_o is the equilibrium temperature, which cannot be determined by means of calorimetric techniques, since for the transformation to take place, a further cooling is needed in order to overcome the opposing non-chemical energies, as required by the transformation kinetics. This temperature can be estimated using the Tong and Wayman approximation [14, 15] which is the most widely accepted for the thermoelastic martensitic transformation

$$T_o = 1/2(M_s + A_f) \quad (6)$$

By subtracting Equations 3 and 4 and bearing in mind that $E_{frA\to M} = E_{frM\to A}$, the elastic energy is obtained as

$$\Delta H_{el} = \Delta H_{chem} - \bar{Q} \quad (7)$$

where $\bar{Q}$ is the average heat measured experimentally in both processes. The friction energy can be obtained by adding Equations 3 and 4. The most accurate method, however, evaluates the above energy as the area within the hysteresis cycle (normalized entropy versus temperature).

3. Results and discussion

The grain size values obtained (perimeter, area and average diameter) are shown in relation to heat treatment time and for each testing temperature in Fig. 1, 2 and 3 for each growth parameter. As expected, on raising the temperature the kinetics growth rate is faster and on extending the period of time at the same temperature, grain growth increases.

These graphs show that rapid grain growth occurs during the first minutes of heat treatment, but subsequently, the growth rate decreases. This slow grain growth, with a practically constant grain size after 60 min of continuous heat treatment, is due to a decrease in the grain boundary surfaces and as a consequence of the decrease in the driving force [16]. Besides, grain growth is prevented by a kinetic impediment due to either the accumulation of impurities and defects or to the lack of continuity in the solid, even if thermal energy is applied.

The grain growth kinetics of the alloy follows the Arrhenius type equation given in Equation 1. This kinetic process defines a linear relationship between $\log D$ and $\log t$, the slope of which gives the growth exponent n. The results obtained from the calculations are shown in Table I.

At 900 °C the growth order is about 0.45, which is high when compared to that of other metals and alloys. In the ideal case the growth order would be 0.5, but generally n is observed to be less than 0.5 due to the role played by different grain growth parameters, such as impurity drag, free surface effect, textured materials and dislocation substructure [17, 18].

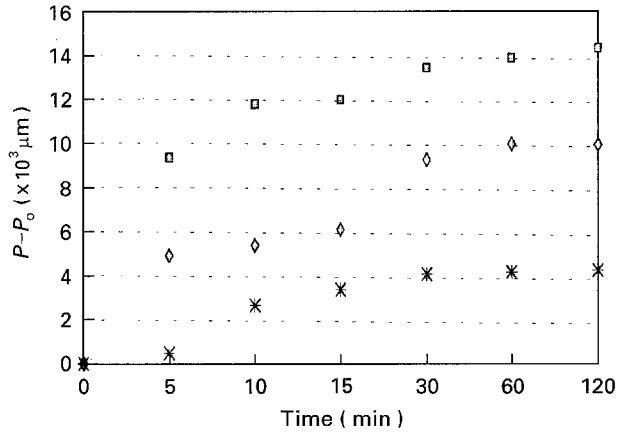

Figure 1 Perimeter in relation to heat treatment time and at each test temperature: (∗) 900 °C, (◇) 1000 °C, and (□) 1100 °C.

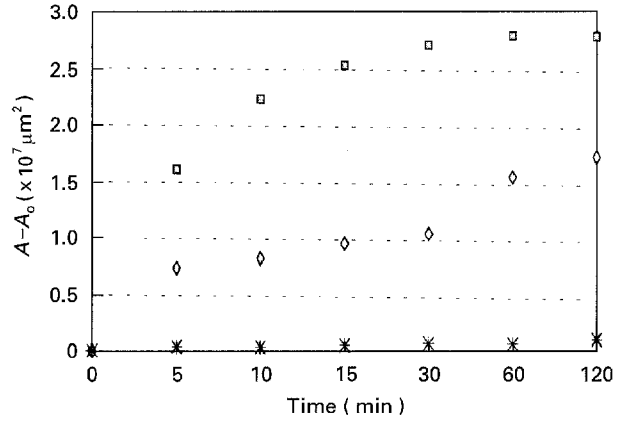

Figure 2 Area in relation to heat treatment time and at each test temperature: (∗) 900 °C, (◇) 1000 °C, and (□) 1100 °C.

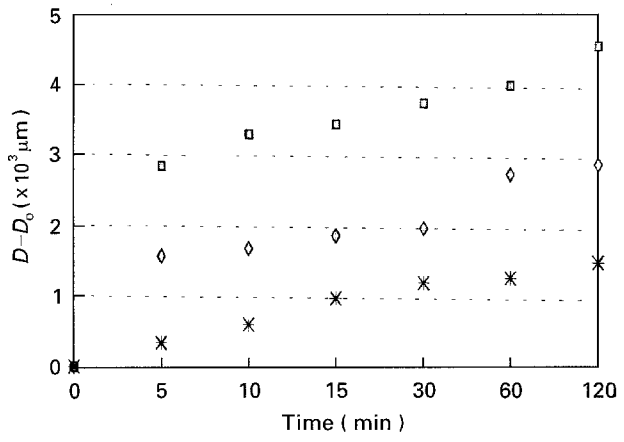

Figure 3 Diameter in relation to heat treatment time and at each test temperature: (∗) 900 °C, (◇) 1000 °C, and (□) 1100 °C.

Usually, n remains constant or increases with increasing temperature. The growth order at 1100 °C and 1000 °C ranges from 0.15 to 0.28 for the three parameters. The differences observed in relation to other alloys are caused by a discontinuity at the phase transition at the different test temperatures. At 1100 and 1000 °C, the parent phase of NiTi has a body centred cubic B2 structure like that of CsCl ($a_0 = 0.301$–0.302) [19], but at 985 °C the parent phase partially transforms into a δ phase with a face centred cubic structure [20].

TABLE I Grain growth equations and growth orders, n, for the heat treatment temperatures and times tested (r is the correlation coefficient)

Parameter	Equation	n	r
At 900 °C			
Perimeter	$\log P - P_0 = 2.75 + 0.48 \log t$	0.48	0.80
Area	$\log A - A_0 = 5.12 + 0.43 \log t$	0.43	0.99
Diameter	$\log D - D_0 = 2.38 + 0.42 \log t$	0.42	0.92
At 1000 °C			
Perimeter	$\log P - P_0 = 3.50 + 0.25 \log t$	0.25	0.93
Area	$\log A - A_0 = 5.65 + 0.28 \log t$	0.28	0.98
Diameter	$\log D - D_0 = 3.03 + 0.20 \log t$	0.20	0.97
At 1100 °C			
Perimeter	$\log P - P_0 = 3.86 + 0.17 \log t$	0.17	0.96
Area	$\log A - A_0 = 7.09 + 0.22 \log t$	0.22	0.95
Diameter	$\log D - D_0 = 3.35 + 0.15 \log t$	0.15	0.98

TABLE II Activation energies for the different grain size parameters

Parameter	Q (kJ mol^{-1})
Perimeter	30
Area	35
Diameter	28

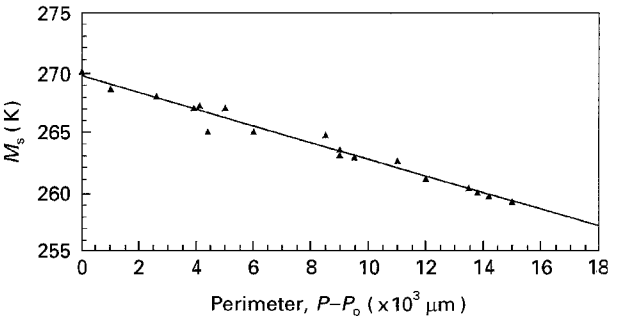

Figure 4 M_s transformation temperature versus perimeter growth.

The authors hypothesize that the diffusion of solute atoms induces the grain boundary migration: this process leads to solution depletion at the grain boundaries and to an increase in the rate of growth [17].

The activation energy has been calculated as the slope of the straight line adjusted from $\log D$ and $1/2$, $3RT$. Table II shows the results which range between 28 and 35 kJ mol^{-1}.

These energies are lower in relation to other shape memory alloys, such as Cu–Zn–Al, with activation energies of approximately 90 kJ mol^{-1} [21], or when compared to other conventional metallic systems, like Fe in α-Fe, where the value is 239 kJ mol^{-1} [22], or for Ti–6Al–4V where it is 95 kJ mol^{-1} [23]. This means that the grain growth process in NiTi is more favoured thermodynamically than kinetically. Thus the kinetic factor acts as a grain growth impediment because the decrease in the grain growth order is sharp in relation to the temperature in the NiTi alloy.

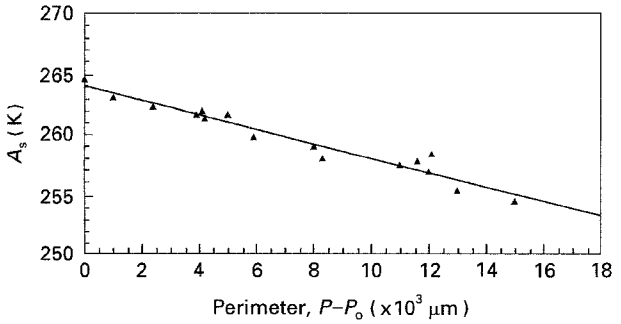

Figure 5 A_s transformation temperature versus perimeter growth.

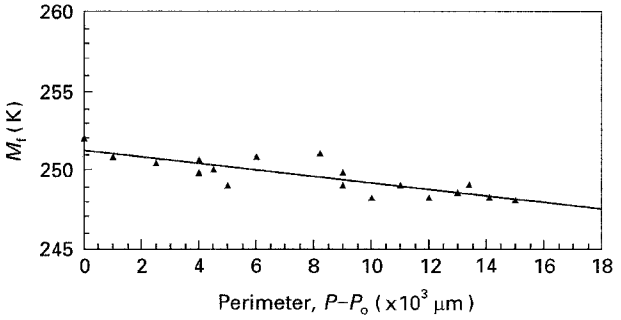

Figure 6 M_f transformation temperature versus perimeter growth.

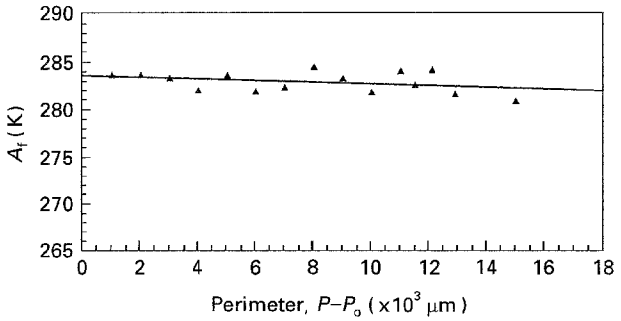

Figure 7 A_f transformation temperature versus perimeter growth.

The transformation temperatures M_s, M_f, A_s and A_f were obtained from the calorimeter graphs. It should be pointed out that the thermograms correspond to the burst type transformation.

The M_s and A_s temperatures, which correspond to the start of the martensitic transformation and retransformation, are shown in relation to the grain size in Figs 4 and 5, respectively. Both temperatures show the influence of grain boundaries, which favour the martensitic transformation and at the same time obstruct the retransformation.

When the martensitic plates interact with the grain boundaries, new martensitic plates nucleate and propagate in the neighbouring grain. Therefore, as the grain size decreases, the grain boundary area increases and the nucleation sites also increases. This interaction produces an increase in the local elastic energy which facilitates the nucleation of new plates. Therefore, samples with small crystals will have greater internal stresses, where the relative anisotropy of the grains will also help the martensitic transformation. Consequently, the M_s temperature for samples with small grain size will be greater than the M_s temperature for samples with large grain size [24–26].

TABLE III Enthalpies and entropies associated with the austenite ⇄ martensite transformation and retransformation

$\Delta H^{A\to M}$ (J g^{-1})	$\Delta H^{M\to A}$ (J g^{-1})	ΔH (J g^{-1})	$\Delta S^{A\to M}$ (J g^{-1} K^{-1})	$\Delta S^{M\to A}$ (J g^{-1} K^{-1})	ΔS (J g^{-1} K^{-1})
11.72	− 12.24	11.98	0.0405	− 0.0452	0.0429

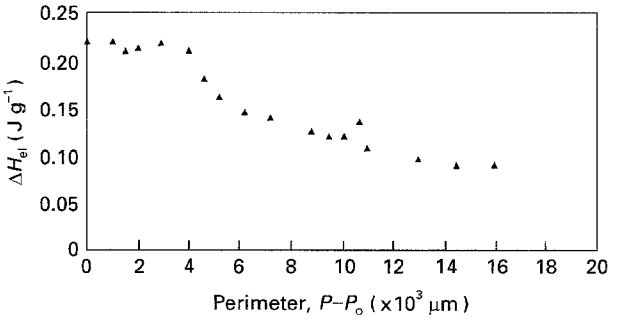

Figure 8 Elastic energy variation in relation to the perimeter growth.

The A_s temperature of the sample with small grain size is greater than that of the sample with large grain size; this is caused by the martensitic plates disappearing in the same way in which they appear. A great deal of energy must be applied in order to separate the plates from the grain boundaries [24, 25].

M_f and A_f temperatures are almost constant with grain size, as shown in Figs 6 and 7.

The transformation temperature range, M_s–M_f, stays around values of 15 from 18 K, but when the perimeter increases it drops down to 10 K due to the M_s decrease and the fact that that stays around M_f is practically constant. The retransformation temperature range, A_f–A_s stays around values of 20 K, but when the grain size increases, it reaches 29 K. This fact is explained in the same way as for M_s–M_f: the A_s temperature drops down and A_f is practically constant.

When the thermograms are analysed, the area under the curve represents the heat exchanged during the transformation, which is considered to be a good representation of the enthalpy variation, ΔH. Other contributions to the heat exchange (elastic, interfacial and dissipative) are comparatively small [27, 28]. The entropy of transformation can be obtained by integration of the corrected thermal power divided by the instantaneous temperature.

The transformation and retransformation average values of enthalpy and entropy, respectively, of all the grain sizes studied are given in Table III. The results show that within the experimental errors, the enthalpy and the entropy changes are independent of grain size. Moreover, there are systematic differences between the absolute values of the enthalpies and the entropies for forward (austenite → martensite) and reverse (martensite → austenite) transformation.

The equilibrium temperature was taken from the approximation described in Equation 6 and the elastic

and chemical energies were calculated by Equations 5 and 7. From these calculations, the relationship between elastic energy and grain size parameter (perimeter) was obtained, as can be seen in Fig. 8. The thermodynamic analysis shows that the elastic energy decreases with grain growth. This fact may reveal that bigger plates grow in the samples with large grain size.

The interpretation may be that martensitic plates growing between grain boundaries produce a lower elastic energy increase than when the grain size is small.

Acknowledgements

The authors acknowledge Dr J. Muntasell and Dr J. Font, Departamento de Física (ETSEIB), in Universidad Politécnica de Cataluña, Spain, the facilities given to use the flow calorimeter.

References

1. F. J. GIL, PhD thesis, Universidad de Barcelona (1989).
2. J. MUNTASELL, J. L. TAMARIT, E. CESARI, J. M. GUILEMANY and F. J. GIL, *Mater. Res. Bull.* **24** (1989) 445.
3. P. J. BROFMAN and G. S. ANSELL, *Metall. Trans.* **14A** (1983) 1929.
4. S. KAJIWARA, *ibid.* **17A** (1986) 1693.
5. P. A. BECK, J. C. KREMER, L. S. DEMER and M. L. HOLZWORTH, *Trans. Met. Soc. AIME* **175** (1948) 507.
6. P. A. BECK, *J. Appl. Phys.* **19** (1948) 507.
7. P. A. BECK, J. TOWERS and W. O. MANLEY, *Trans. Met. Soc. AIME* **185** (1951) 634.
8. G. T. HIGGINS, *Met. Sci.* **8** (1974) 143.
9. B. RALPH, *Mater. Sci. Technol.* **6** (1990) 1139.
10. J. ORTÍN and A. PLANES, *Acta Metall.* **36** (1988) 1873.
11. J. M. GUILEMANY and F. J. GIL, *Mater. Res. Bull.* **25** (1990) 1352.
12. A. G. GUY and J. J. HREN, "Elements of Physical Metallurgy", 3rd edn (Addison–Wesley, Massachusetts, 1974) p. 446.
13. D. N. ADNYANA, in "Proceedings of the International Conference on Martensitic Transformation, ICOMAT-86" (The Japan Institute of Metals, Naru, 1986) p. 774.
14. C. M. WAYMAN and H. C. TONG, *Scripta Metall.* **11** (1977) 341.
15. H. C. TONG and C. M. WAYMAN, *Acta Metall.* **22** (1974) 887.
16. M. HILLERT, *ibid.* **13** (1965) 227.
17. G. T. HIGGINS, *Met. Sci.* **8** (1974) 143.
18. R. ELST, J. VAN HUMBEECK and L. DELAEY, *Z. Metallkde* **76** (1985) 705.
19. K. SHIMIZU and T. TADAKI, in "Shape Memory Alloys", edited by H. Funakubo (Gordon & Breach, Tokyo, 1984) p. 19.
20. D. KOSKIMAKI, M. J. MARCINKOWSKI and A. S. SASTRI, *Trans. Met. Soc. AIME* **245** (1969) 1883.
21. J. M. GUILEMANY and F. J. GIL, *J. Mater. Sci.* **26** (1991) 4626.
22. R. L. FULHMAN, "Interfaces Seminar" (American Society for Metals, Metals Park, OH, 1952) p. 179.
23. F. J. GIL and J. A. PLANELL, *Scripta Metall. Mater.* **25** (1991) 2843.
24. J. M. GUILEMANY and F. J. GIL, *Thermochim. Acta* **167** (1990) 136.
25. *Idem, J. Mater. Sci.* **9** (1974) 1545.
26. *Idem, J. Mater. Sci. Lett.* **12** (1993) 6.
27. J. ORTÍN and A. PLANES, *Acta Metall.* **36** (1988) 1873.
28. C. M. FRIEND, J. ORTÍN, L. MAÑOSA and M. YOSHIKAWA. *Scripta. Metall. Mater.* **24** (1990) 1641.

Received 4 July
and accepted 25 November 1994